Correlated Random Walk of tuna in arrays of Fish Aggregating Devices: A field-based model from passive acoustic tagging

Géraldine Pérez, Amaël Dupaix, Laurent Dagorn, Jean-Louis Deneubourg, Kim Holland, Sunil Beeharry, Manuela Capello

Ecological Modelling
August 2022, Volume 470 Pages 110006 (12p.)
https://doi.org/10.1016/j.ecolmodel.2022.110006
https://archimer.ifremer.fr/doc/00770/88237/

Correlated Random Walk of tuna in arrays of Fish Aggregating Devices: A field-based model from passive acoustic tagging

Pérez Géraldine [1, *], Dupaix Amael [1], Dagorn Laurent [1], Deneubourg Jean-Louis [2], Holland Kim [3], Beeharry Sunil [4], Capello Manuela [1]

[1] MARBEC, Univ Montpellier, CNRS, Ifremer, IRD, Sète, France
[2] Unit of Social Ecology, Université Libre de Bruxelles (ULB), Bruxelles, Belgium
[3] Hawai'i Institute of Marine Biology at University of Hawai'i, Kane'ohe, Hawai'i, United States of America
[4] Ministry of Ocean Economy, Marine Resources, Fisheries and Shipping, Mauritius

* Corresponding author : Géraldine Pérez, email address : geraldine.perez@ntymail.com

Abstract :

For centuries fishers have exploited the propensity for tuna to associate with floating objects, yet the reasons and mechanisms behind this behavior remain unclear. The number of man-made floating objects (FADs, Fish Aggregating Devices) undergone a dramatic increase in recent decades, with the development of industrial tuna purse seine fishing. However, current knowledge does not allow for the evaluation of the consequences of this increase on the ecology of tuna. Here, we developed a model of tuna movements in an array of FADs, using passive acoustic tagging data. The model was built using four behavioral rules: (1) when no FAD is perceived, tuna exhibit a random search behavior, (2) individuals can orient directly to a FAD when they perceive it (within a given orientation radius), (3) the associative dynamics of tuna follow a daily rhythm and (4) Continuous Residence Time (CRTs – time spend at FAD by tuna) are independent from previous Continuous Absent Time (CATs- time between two consecutive CRTs). The model is based on only four parameters: swimming speed, path sinuosity, orientation distance and a loss term to account for natural and fishing mortality events. The model was calibrated on 70±10 cm yellowfin tuna (Thunnus albacares), acoustically tagged in two different networks of anchored FADs (Oahu, Hawaii, U.S.A. and Mauritius) with different FAD densities. Our results show that the model can reproduce the time tuna spent traveling between FADs (i.e., time away from the FADs), as well as the total time spent by the fish in the FAD array (total residence time) at both study sites. The parameter sets that best reproduce the experimental data correspond to a steering radius between 2 and 5 km, a sinuosity (correlated random walk parameter) between 0.9 and 0.995 and mortality rates between 1 and 3% per day. This model, thus parameterized, could be used in future studies to predict tuna movements in arrays of different FAD densities and thus provide scientific advice for their management. The same approach can be used for modeling the movements of marine and terrestrial animals detected near aggregation sites.

Highlights

► First model to reproduce tuna movements in an array of Fish Aggregating Device. ► Calibration of the model parameters using passive acoustic telemetry data. ► This model can be used to evaluate the impact of increasing numbers of aggregation sites on the movement behavior of animals.

Keywords : Correlated Random Walk, Tropical tuna, Spatial model, Fish Aggregating Device, Acoustic tagging, Survival curve, Tuna motion, Residency

1. Introduction

With more than 5.3 million tonnes caught in 2019 (ISSF, 2021) tropical tuna constitutes one of the major harvested fish species. Currently, yellowfin tuna (*Thunnus albacares*), bigeye tuna (*T. obesus*) and skipjack (*Katsuwonus pelamis*) represent almost 95% of the global tuna catches (ISSF, 2021). Tropical tunas display an associative behavior with floating objects, forming large multi-specific aggregations around them. The reasons why tuna associate with floating objects are still unknown. Two main hypotheses are widely accepted: (1) the meeting-point hypothesis (Dagorn & Fréon 1999, Fréon & Dagorn, 2000) and (2) the indicator-log hypothesis (Hall, 1992). The meeting-point hypothesis posits that floating objects act as meeting-points, where tuna gather to form bigger schools. The indicator-log hypothesis posits that natural floating objects, such as logs, are more numerous in productive areas , as they concentrate in river months, estuaries and frontal structures. Following this hypothesis, tuna could use floating objects as indicators of productive areas.

Fishers have used this associative behavior to their advantage for centuries (Dempster & Taquet, 2004) and, more recently, have deployed human-made floating objects, called Fish Aggregating Device (FAD), to increase their catches. In the open ocean, drifting FADs are primarily used by industrial purse seine fleets, while, in coastal areas, anchored FADs are used by artisanal and semi-industrial fisheries (Dagorn et al. 2013b; Dempster & Taquet, 2004; Scott & Lopez, 2014). About 37% of the tropical tuna catches (all fishing gears) are made by purse seiners on drifting FADs, ranging between 32% to 51% depending of the ocean (Dagorn et al. 2013b; Murua et al. 2021). The number of FADs has drastically increased in the three past decades, with more than 100,000 FADs deployed globally, each year (Scott & Lopez, 2014), although precise numbers are difficult to obtain.

This increase raised concerns over possible impacts on tuna populations, because FADs increase the vulnerability of tunas to capture but also because increasing the number of floating objects (Dagorn et al. 2013b) could affect their ecology. Marsac et al. (2000), were the first to suggest that FADs could act as an ecological trap for tunas. Following the indicator-log hypothesis, FADs could mislead tuna if they are deployed or drift into biologically poor areas and if tuna do not differentiate between natural and man-made objects. Therefore, tuna could remain associated with FADs even if their surrounding environment is detrimental to their fitness (Marsac et al. 2000). However, current knowledge does not allow for the assessment of the effects of increasing FAD densities on tuna ecology, even when the environment (other than floating objects) remains constant.

Acoustic telemetry has been widely used to monitor tuna movements and behavior within FAD arrays. With this technology, acoustically tagged fish (i.e., fish equipped by an acoustic tag) can be either actively tracked or detected by a set of fixed acoustic receivers. In the former case, known as *active tracking*, the recorded path of the receiver, which is considered as a proxy of the animal path, generally corresponds to short periods of time (few days at most) (Girard et al. 2004; Girard et al. 2007). In the latter case, known as *passive acoustic telemetry,* a time series of acoustic detections is recorded within the array of receivers (Dagorn et al. 2007; Tolotti et al. 2020). The acoustic receivers are generally placed in proximity of aggregation/attraction sites (FADs in this case), where it is more likely to detect the tagged individuals. Passive acoustic telemetry has the advantage to cover longer period of time (up to several months or even more than a year, depending on the tag battery life and the fish residency within the array). However, the time series of acoustic detections recorded at aggregation sites cannot be easily translated into movement rules.

Previous passive acoustic telemetry studies conducted in anchored FAD arrays quantified the amount of time that tuna spend associated with these floating objects (residence times), as well as the time they spend traveling between two objects (absence times) (Dagorn et al. 2007; Govinden et al., 2013; Robert et al., 2013; Rodriguez-Tress et al., 2017). These studies highlighted the variability of such durations according to both the size of the tagged individuals (Robert et al., 2013) as well as the species (Rodriguez-Tress et al., 2017). Recently, Pérez et al. (2020) compared the residence and absence times recorded for individual tuna tagged within different FAD arrays, demonstrating that tuna spend less time traveling between FADs and more time in association as FAD density increases. Passive and active acoustic telemetry studies have also shown a diel rhythm in the associative behavior of tunas, with close association occurring mostly during the daytime while regular excursions away from the FAD are undertaken at night (Holland et al. 1990; Marsac & Cayré, 1998; Dagorn, et al. 2000; Forget et al., 2015; Tolotti et al., 2020). Furthermore, active tracking studies allowed the fine-scale movements of tagged individuals in arrays of FADs to be investigated. Using acoustic telemetry data from actively tracked yellowfin tuna in anchored FAD arrays in the Pacific

and Indian oceans, Girard et al. (2004) found that tuna adopt a random search behavior until they perceive a FAD, then orient towards the device at distances ranging between 4 to 17 km.

Recently, Pérez et al. (2020), used a simple random walk model to assess whether the observed trends in behavioural indices, obtained from passive acoustic tagging data across increasing FAD densities, could result from the random-search component in tuna behaviour suggested in previous experiments (Girard et al. 2004). While this simple model was able to explain the observed trends of shorter absence times for increasing FAD densities, it could not quantitatively predict their durations, since it did not account for the oriented movements (Girard et al. 2004) or for the diel pattern in tuna behavior (Marsac & Cayré, 1998; Forget et al., 2015). Correlated Random Walk (CRW) models are frequently used to reconstruct animal paths from active tracking data (e.g. Girard et al. 2004; Patterson et al. 2009; McClintock et al. 2012; Cramer et al. 2021), as well as to simulate their movements (Byers, 2001; Carita et al. 2012; Ahearn et al. 2017; Cramer et al. 2021). These models are used because, unlike a simple random walk, they account for the tendency of animals to go forward. A CRW model is thus a better choice than a simple random walk for animals with bilateral symmetry such as tuna. On the other hand, despite the large availability of passive acoustic telemetry data for tuna and their large temporal coverage, this data has not been used so far to construct this type of models, due to the discrete nature of the data (acoustic detections) recorded both in time and space.

The aim of this study was to develop a data-based model of tuna movements in an array of FADs, which can reproduce the motion of tuna from one FAD association to another detected through passive acoustic telemetry. Such model constitutes the first step to predict the effects of increasing FAD numbers on tuna behavior and ecology. The model was calibrated using passive acoustic telemetry data collected at two study sites (Mauritius, see Rodriguez-Tress et al. 2017, and Oahu, Hawaii, U.S.A., see Dagorn et al. 2007; Robert et al. 2013) with different FAD densities (Pérez et al. 2020).

2. Materials & Methods

2.1. Field data

Passive acoustic telemetry data were used to characterize tuna movements in FAD arrays. This technology is based on the transmission of an acoustic signal between an acoustic transmitter (or tag) implanted in a tuna and acoustic receivers (or hydrophones) installed at specific study sites. The identification of the tagged fish is possible when the fish is located close to the receivers, within a given detection range. Passive acoustic tagging data were collected in two anchored FAD arrays, one around the island of Mauritius (Rodriguez-Tress et al. 2017) in the Western Indian Ocean, and the

other around the island of Oahu (Robert et al. 2013), within the Hawaiian archipelago in the Central Pacific Ocean (Fig. 1). These anchored FAD arrays differ in their inter-FAD distances, with the Mauritian array having shorter nearest and next-nearest neighboring distances than the Hawaiian array (Pérez et al., 2020). The Mauritian array consisted of 9 FADs with 7 equipped with acoustic receivers, and the Hawaiian array comprised 13 FADs, all of which were equipped with acoustic receivers (see Dagorn et al. 2007; Rodriguez-Tress et al. 2017 for specifications of acoustic receivers). In both arrays, FADs were moored in depths of between 1000 and 2500 m. The design of FADs was similar within the same array, but differed slightly between arrays.

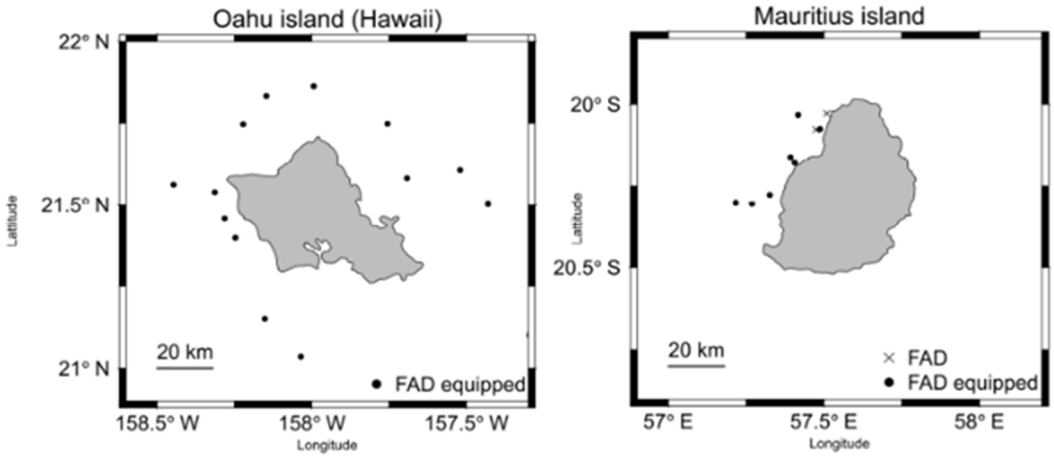

Fig. 1*: Anchored FAD arrays of Mauritius (left) and Oahu (right). Positions of the anchored FADs are represented by a black dot when equipped with an acoustic receiver, and by a black cross otherwise.*

Since previous studies outlined species and size-dependent variability in the associative behavior of tuna at FADs (Robert et al. 2013; Rodriguez-Tress et al. 2017; Pérez et al., 2020), this study focused on a single species (yellowfin tuna) and size of ~70 cm fork length (fork length range: 60-80 cm), named YFT-70, which was common to both study sites. For the Mauritian array, due to the short duration of the experiment (Rodriguez-Tress et al. 2017), the data recorded during the first 38 days was considered, resulting in the smallest observation time. For the Hawaiian array, where the experiment lasted more than one year, only the initial 120 days after tagging were considered because 95% of the time between the first and the last detection at a FAD lasted less than 120 days (Robert et al. 2013). As a result, the field data consisted of 14 YFT-70 tagged in the Mauritian array and 56 YFT-70 individuals in the Hawaiian array (Table 1). Details on the tagging procedures can be found in Rodriguez-Tress et al. (2017) for the Mauritian array and in Robert et al. (2013) for the Hawaiian array.

***Table 1**: Number of yellowfin tuna of ~70 cm tagged (N_{tuna}), total number of CRTs (excluding the first CRT, NCRT) and total number of CAT_{diff} ($NCAT_{diff}$) recorded in the Mauritian and the Hawaiian array.*

	Hawaii	**Mauritius**
N_{tuna}	56	14
NCRT	111	29
$NCAT_{diff}$	59	19

164

165 **2.2. Residence and absence times in the FAD array**

166 Acoustic telemetry data were processed to obtain information on durations of presence at and absence
167 from instrumented FADs displayed by tagged tuna, following the procedure described in Capello et
168 al. (2015). This procedure translates the discrete time series of acoustic detections into continuous
169 bouts of time. It relies on the definition of a maximum blanking period (MBP), i.e., a maximum
170 temporal separation between two subsequent acoustic detections at the same FAD (or receiver), where
171 fish is still considered to be associated. The definition of a MBP not only allows to account for small
172 data gaps related to detection issues and sonic collisions (Forget et al. 2015), but also for fish
173 excursions out of the detection range of the receiver. In the case of tropical tuna, a MBP value of 24h
174 was chosen, in order to account for the regular diel excursions that tuna perform out of the FAD at
175 nighttime (Holland et al. 1990; Marsac & Cayré, 1998; Dagorn et al. 2000; Forget et al. 2015).
176 Following this procedure, the Continuous Residence Times (CRTs) (Ohta & Kakuma 2005; Dagorn
177 et al. 2007; Capello et al. 2015), corresponded to continuous bouts of time spent at the same FAD
178 without any day-scale absence (>24h). Conversely, the time spent away from FADs were defined as
179 Continuous Absence Times (CAT) (Govinden et al. 2013; Capello et al. 2015). Absence times related
180 to movements between two different FADs were referred to as CAT_{diff} (Pérez et al. 2020). Finally, for
181 each individual, the sum of all recorded CRTs and CATs corresponded to the Total Residence Time
182 (TRT), namely the time between the first and the last detection recorded in the FAD array (Fig. 2).

183

184 **2.3. Model**

185 The model was built upon four behavioral rules, based on the current knowledge of the associative
186 behavior of tuna at FADs (Fig. 3): (1) Tuna display a random search behavior between two FAD
187 associations (Girard et al. 2004; Pérez et al. 2020), (2) at a certain distance from FADs tuna show
188 oriented movements towards FADs (Girard et al. 2004), (3) the tuna association dynamics follows a
189 diel rhythm (Holland et al. 1990; Marsac & Cayré 1998; Dagorn et al. 2000; Forget et al. 2015; Tolotti

et al., 2020; Govinden et al. 2021), and (4) CRTs were independent from previous CATs (Robert et al. 2013).

As tuna, like most animals, have a tendency to move forward, the random-search movements were simulated using a Correlated Random Walk model (Kareiva & Shigesada, 1983; Carita et al. 2000; Codling et al. 2008; Ahearn et al. 2017). These models are based on a Markov process where consecutive changes in the animal's consecutive direction are correlated. For each time step Δt, the position of an individual at time t depends on its previous position at time t-Δt and the turning angle α, defining the change in direction relative to the previous time step. Turning angles were randomly sampled from a normal distribution defined in the range $[-\pi; \pi]$, with zero mean and standard deviation σ following the method of Bovet & Benhamou (1988), using the scipy.stats.truncnorm python function. Standard deviation $\sigma = 0$ correspond to straight trajectories whereas in the limit $\sigma \to \infty$ the model converges to a simple random walk. In the following, σ was expressed in terms of the coefficient of sinuosity (c) according to the relationship, $\sigma = \sqrt{(-2\ln(c))}$ with $c \in]0,1]$ (Bovet & Benhamou, 1988; Benhamou 2004). The limit $c \to 0$ corresponds to a simple random walk (highest sinuosity) whereas increasing c decreases the sinuosity, with straight trajectories for c=1. A total of 9 coefficients of sinuosity were tested, ranging between 0.2 and 0.9999 (Table 2). Fig. 4 illustrates the distribution of turning angles and an example of a tuna trajectory for each coefficient of sinuosity tested.

Table 2*: Model parameters that gives the 648 sets of parameters tested.*

Parameters		Values
	Tested parameters	
v	Speed (m/s)	0.7, 1.4
m	Rate of mortality (%/day)	0, 1, 2, 3, 4, 5
R_o	Orientation radius (km)	0, 2, 5, 10, 15, 20
c	Coefficient of sinuosity	0.2, 0.7, 0.9, 0.97, 0.99, 0.995, 0.997, 0,999, 0.9999
	Fixed parameters	
Δt	Time step (s)	100
N	No. of simulated individuals	1000
T	Total duration (day)	38 (Mauritius), 120 (Hawaii)

In order to account for the orientation behavior of tuna towards FADs, different values of the orientation radius were tested (Fig. 4, Table 2 and Supplementary Information 1). Each time a tuna enters within this radius, its path changes to a straight trajectory oriented towards the FAD location. If the tuna was located within the orientation radius of multiple FADs, a FAD was randomly selected between them using a uniform distribution. A total of six orientation radii were tested, ranging between 0 (no orientation) to 20 km, see Table 2. The diel rhythm in the associative behavior of tunas was accounted for by defining two behavioral modes ("daytime" and "nighttime") with a periodicity of 24 hours each. During the 12 hours of "daytime" tuna displayed an orientation behavior towards FADs (if located within the orientation radius). Conversely, during the 12 hours of "nighttime" tuna did not exhibit a long-range attraction to FADs (no oriented behavior within the orientation radius) and therefore followed a simple CRW dynamic. In both "daytime" and "nighttime" behavioral modes a tuna was, however, considered to be associated with a FAD when it was located within 500 m of it. This value is in accordance with both the observations of tuna when they were associated with FADs (see Josse et al. 2000; Moreno et al. 2007), and the detection range of acoustic tags used in telemetry studies around instrumented FADs (see Forget et al. 2015).

The model did not represent the association time of tuna at FADs (CRT), but these durations were needed to compare the model with the field data. Therefore, the CRTs recorded from field data were used as a model input. Each time a tuna reaches a FAD (i.e., it was located within 500 m of it), a CRT value was randomly sampled from the actual CRT data of the corresponding array and the simulated individuals do not move away from the FAD during the entire duration of the CRT. The CRTs recorded from field data in each array are shown in the Supplementary Information 2. Once this time has elapsed, individuals could leave the FAD in a random direction sampled from a uniform distribution between $[-\pi; \pi]$. To avoid immediate returns, during the 24 hours following the end of a CRT, fish was not affected by the association radius (R_o) of the FAD of departure. Similarly, returns due to tuna re-entering the detection range within 24 hours (which were already taken into account in the CRT duration) were neglected. For this purpose, each time a CAT_{return} of less than 24 hours was recorded after a CRT, this movement was discarded and the simulation time was reset to the end of the last CRT recorded (Fig. 3). This procedure ensured that CRT durations were consistent with field data. Since the CRTs recorded immediately after tagging were significantly longer than the other CRTs in the Hawaii field experiments and slightly longer in the Mauritius field data, (see Supplementary Information 2) they were not considered in the above procedure. Accordingly, the first CRT were also subtracted from the TRT to ensure data consistency.

Finally, a mortality rate (m) was considered to account for natural and fishing mortality events that may cause the interruption of the acoustic detections for some tagged individuals. For this purpose, a Monte Carlo algorithm was applied where, for each individual and at each time step, a random number

ε was sampled from a uniform distribution in the interval [0,1] and compared with the corresponding mortality rate using a Bernoulli test. A death was accepted for $\varepsilon < m*T$. The constant T depends on the time step Δt and on the temporal units of the mortality rate. Different mortality rates were tested, ranging between 0 and 5% per day (Table 2). For a mortality rate expressed in $days^{-1}$ and Δt in seconds, T= Δt/(3600×24). The upper bound of 5% per day was estimated from survival analyses of field data (see Supplementary Information 3). TRTs values therefore depended on both the CRW dynamics (which affects the number of tuna associations, thus the time at which the last FAD detections occur) and the mortality rates (Fig. 2).

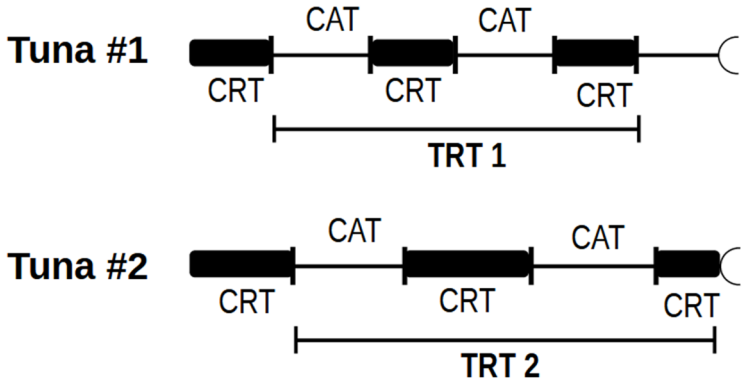

Fig. 2*: Schematic diagram of behavioral sequences and Total Residence Time (TRT) definition. The tuna #1 presents a TRT ending at the end of the last Continuous Residence Time (CRT), recorded before the end of the experiment (indicated by a C-shape). The tuna #2 presents a TRT ending during a CRT because the experiment stopped, while the tuna was associated. CAT corresponds to Continuous Absence Times.*

The model was run in a continuous unbounded space, centered around the actual FAD arrays of Mauritius and Hawaii. The topography of each island was considered using data from the R package "rworldmap" (South 2011). Each time simulated individuals were at risk of crossing island boundaries, the distribution of turning angles α was sub-sampled in order to avoid the island.

A total of 1000 individuals were considered in each FAD array, for each combination of model parameters. For each individual, the simulations started at one of the FADs of tagging, in order to reproduce the experimental design as accurately as possible. The probability to start at a given FAD was obtained considering the number of tuna tagged at the FAD, relative to the total number of tuna tagged in the field experiment (see Supplementary Information 4). Two different swimming speeds were tested: 0.7 and 1.4 m/s, corresponding to one and two body-lengths per second respectively (see swimming speeds in Girard et al. 2004 and tagging studies used in this study: Robert et al. 2013 and Rodriguez-Tress et al. 2017). Time steps (Δt) lasted 100 s and each resulted in individual fish movements of 70 and 140 m depending on the speed.

A summary of all model parameters can be found in Table 2. All the simulations were performed using the Python 3 programming language (Python Software Foundation, version 3.8.5).

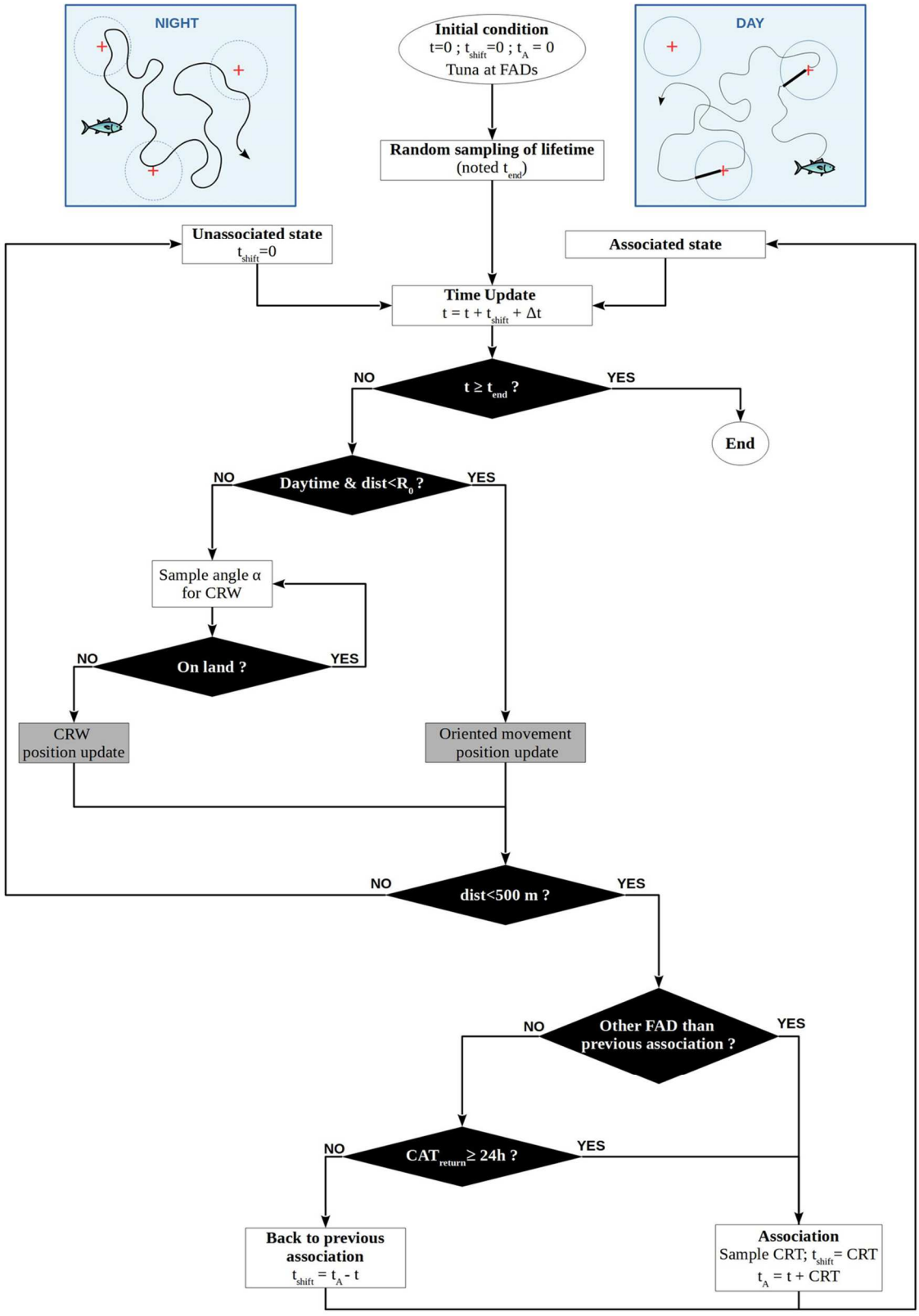

Fig. 3*: Flow-Chart diagram illustrating the model algorithm. CRW denotes Correlated Random Walk, R_0 corresponds to the orientation radius, dist corresponds to the distance between the tuna and*

the closest Fish Aggregating Device (FAD) and the value t_{end} takes into account the death of tuna as well as the end of the experimentation.

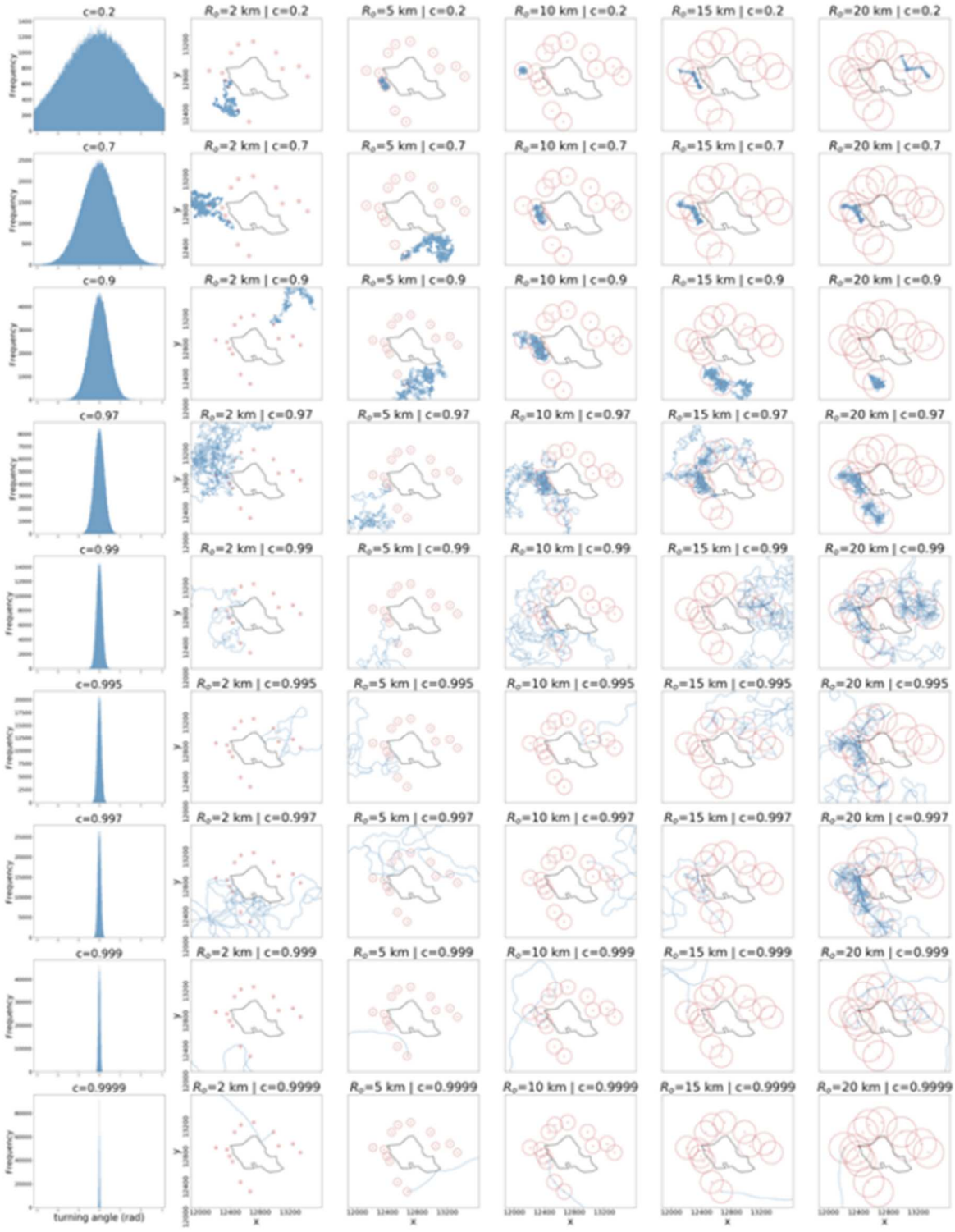

***Fig. 4**: Example of tuna path trajectories according to the coefficient of sinuosity (c; rows) and the orientation radius (R_o, columns) tested for the Hawaiian array. The first column shows the distribution of turning angles (α in radians) for each coefficient of sinuosity tested. The orientation radii are represented by red circles centered around each FAD and the case Ro=0 is not represented. For the Mauritian array, see Supplementary Information 2.*

2.4. Comparison between simulated and field data

Since the model aimed at fitting the time that tuna spent between two FAD associations (CAT_{diff}), the comparison between the model and the field data focused on this metric. However, the distribution of CAT_{diff} also depends on the total time spent in the FAD array (i.e. longer CAT_{diff} can only be observed for longer TRT). As such, the comparison between the model and the field data was performed for both metrics. For this purpose, CAT_{diff} and TRT were obtained from the simulated data using the same procedures applied to the field data. The selection of model parameters which best fitted the field data was made using a survival analysis, by comparing the theoretical survival curves of the TRT and the CAT_{diff} with those obtained from field data, through a bootstrap method. Experimental survival curves S(t) were constructed (Capello et al. 2015), which represented the proportion of events (TRT or CAT_{diff}) longer than a given duration t. For each set of parameters the survival curve of the field data was compared 1000 times with a sub-sample of the same size as the field data, *i.e*. 56 individuals for Hawaii and 14 for Mauritius (Table 1), randomly sampled from the 1000 simulated individuals. For each of the bootstrap sample , survival curves obtained from the simulated and field data were compared using Cox proportional hazards regressions. The statistical significance of the model was assessed using the p-value from a logrank test, which tested the null hypothesis of identical hazards between the model and the field data. For each survival curve (TRT and CAT_{diff}) and FAD array (Mauritius and Hawaii), the percentage of retained bootstrap tests was calculated, corresponding to the number of bootstrap tests showing p-values>0.05 over the 1000 tests performed. Finally, each set of parameters was assigned the lower percentage of retained bootstraps estimated over survival curves (TRT and CAT_{diff}) and FAD arrays (Hawaii and Mauritius).

The Cox proportional hazards regressions and logrank tests were performed using the R software (R Core Team 2018 version 3.4.4) with the function “coxph” in the “survival” package version 3.1-8 (Therneau & Grambsch 2000).

326

327 3. Results

328 A total of 648 sets of parameters were tested (Table 2), of which 7 appeared to best fit both the CAT_{diff}
329 and TRT recorded in the Mauritian and Hawaiian arrays considering a percentage of retained
330 bootstrap tests ≥85% (Table 3 and Supplementary Information 5). That is, over the 1000 tests
331 performed for each set of parameters, 7 sets were not statistically different from the field data in more
332 than 85% of the tests performed on both survival curves (TRT and CAT_{diff}) and FAD arrays (Mauritius
333 and Hawaii). Fig. 5 and Fig. 6 present the CAT_{diff} and TRT survival curves for each FAD array, for
334 the two sets of parameters performing the best.

Table 3: *Set of retained model parameters for which more that 85% of the bootstrap tests fit the field data. .*

v **(m/s)**	***m*** **(%/day)**	R_o **(km)**	**c**	**Retained Bootstraps (%)**
0.7	2	5	0.99	91.5
1.4	2	2	0.97	90.7
1.4	3	2	0.9	89.8
0.7	2	5	0.995	89.7
1.4	4	2	0.9	89.4
1.4	2	2	0.9	87.5
0.7	3	5	0.99	86.6

335

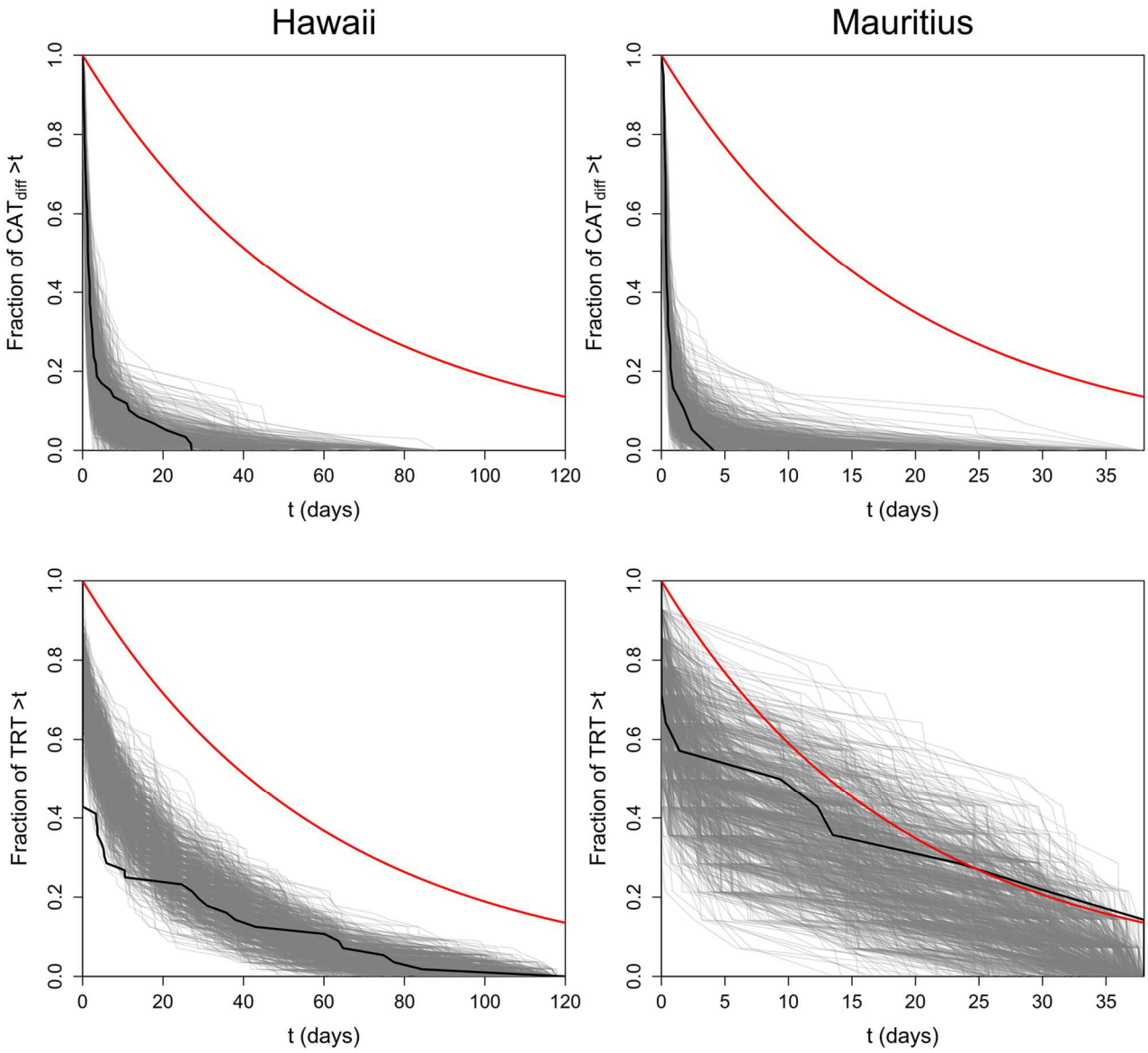

Fig. 5.*: Comparison of survival curves obtained from field data(black) and from the 1000 bootstrap samples (gray) for a speed* ***v=0.7 m s^{-1}****, a mortality* ***m=2%****, a orientation radius* ***R$_o$=5 km*** *and a coefficient of sinuosity* ***c=0.99*** *(with % retained bootstrap =* ***91.5%,*** *see Table 3). The first row corresponds to the survival curves of CAT$_{diff}$ (A and B) and the second row to the TRT (C and D). The first column denotes the Hawaiian FAD array (A and C) and the second column the Mauritian array (B and D). The red line corresponds to the theoretical curve (exp(-mt)) representing the upper bound of TRT.*

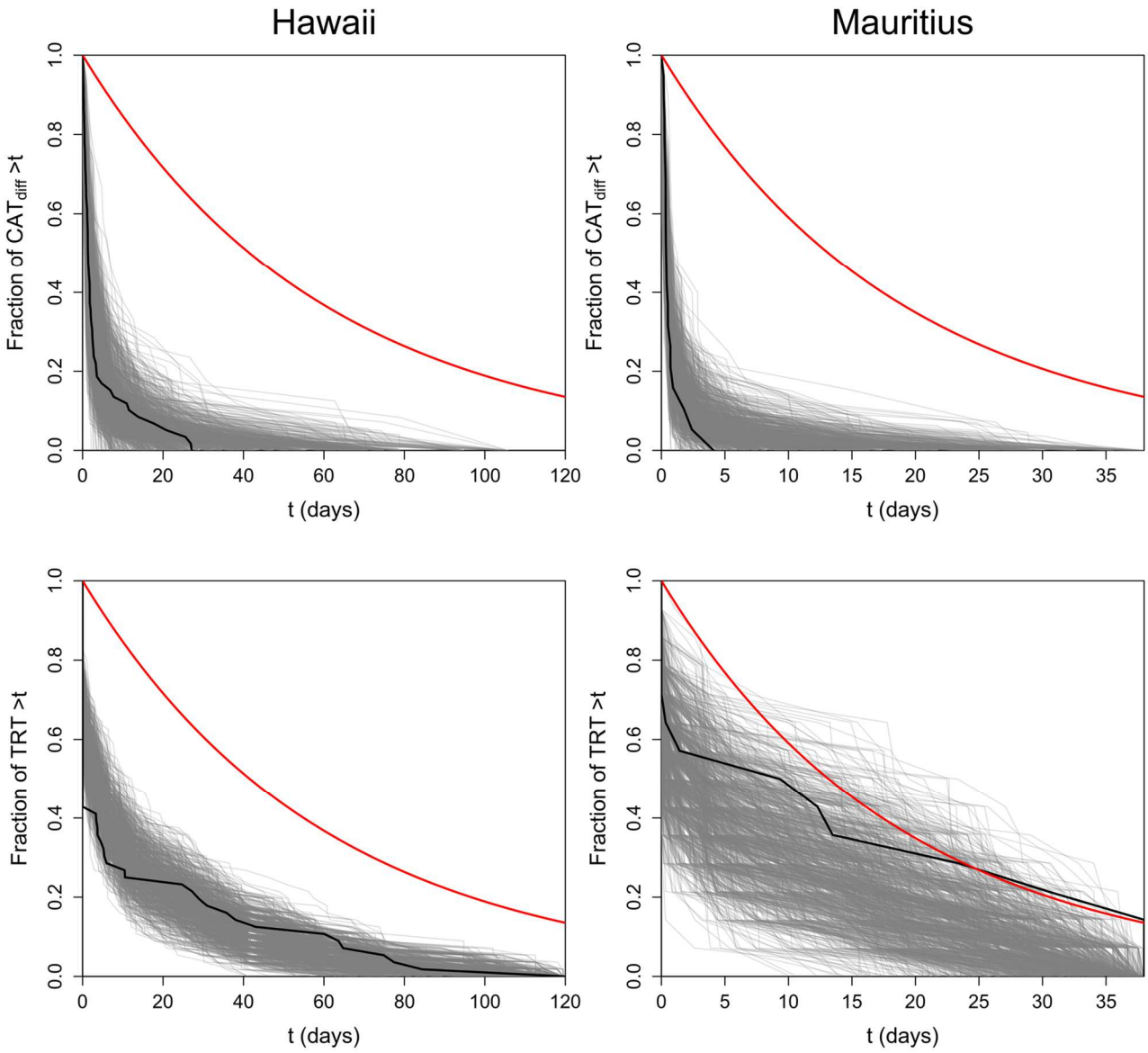

Fig. 6*: Comparison of survival curves obtained from field data(black) and from the 1000 bootstrap samples (gray) for a speed* ***v=1.4 m s^{-1}****, a mortality* ***m=2%****, a orientation radius* ***R$_o$=2 km*** *and a coefficient of sinuosity* ***c=0.97*** *(with % retained bootstrap =* ***90.7%,*** *see Table 3). The first row corresponds to the survival curves of CAT$_{diff}$ (A and B) and the second row to the TRT (C and D). The first column denotes the Hawaiian FAD array (A and C) and the second column the Mauritian array (B and D). The red line corresponds to the theoretical curve (exp(-mt)) representing the upper bound of TRT.*

The complete results of the bootstrap test are available in Supplementary Information 6. Any speed values between the tested ones (0.7 and 1.4 m/s) will reflected the field behavior (Fig. 7 and Supplementary Information 7). In the same way, all values of the mortality rate can be retained. However, null mortalities (m=0), showed poorer bootstrap results (higher percentage of retained bootraps of 62.2%, see Fig. 7, Supplementary Information 6 and 7). Similarly, mortality rates of 5%

and 1% did not appear among the 7 best fits (Table 3). However, combinations of parameters exist with high percentages of retained bootstraps (83.5% for m=5%/day and 80.1% for m=1%/day, see Fig. 7, Supplementary Information 6 and 7). On the opposite, orientation radii of 2 and 5 km clearly stand out (Fig. 7 and Supplementary Information 7)), all the other values having a percentage of retained bootstraps below 55% (Fig. 7, Supplementary Information 6) and even below 20% for orientation radii of 15 and 20 km (Fig. 7, Supplementary Information 6). Finally, the coefficients of sinuosity (c) performing the best range from 0.9 to 0.995 (all with a percentage of retained bootstraps above 80%, Fig. 7, Supplementary Information 6 and 7). Coefficients of c=0.2, 0.999 and 0.9999 showed poorer results (percentage of retained bootstraps respectively 37.2%, 51.3% and 7%, see Fig. 7, Supplementary Information 6 and 7).

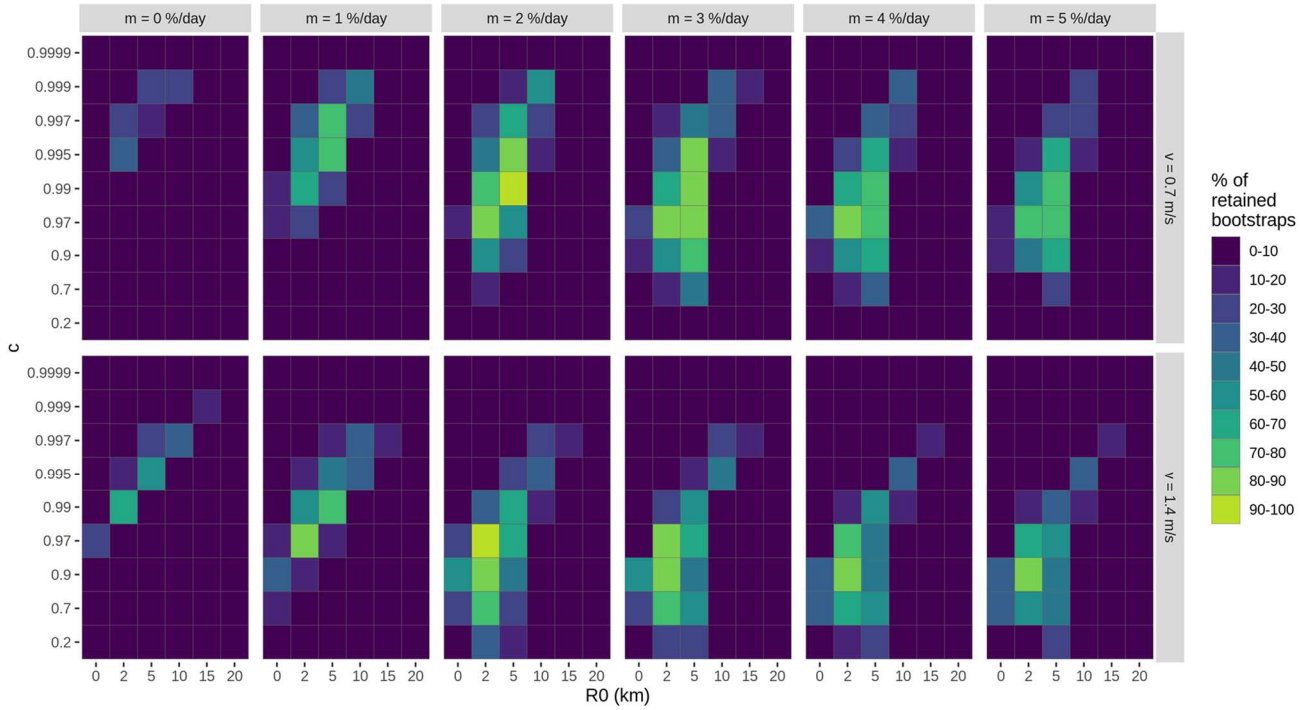

***Fig. 7**: Heatmap of the percentage of retained bootstraps that fit the field data for each set of model parameters. Rows corresponds to the tested speeds (v), columns denote the mortality rates (m). Tested values of the orientation radius (R_0) are shown in the x-axis and tested coefficients of sinuosity (c) in the y-axis.*

4. Discussion

The study of animal behavior made considerable progress in the last decades, thanks to the development of electronic tagging and camera trapping technologies (Swann & Perkins, 2014; Hughey et al. 2018). However, characterizing the movement of animals in their own environment still remains a challenging task, particularly in marine environments, where GPS technologies can rarely

384 be used. Here, through the use a field-based modeling approach and passive acoustic telemetry data,
385 we provide, for the first time, a method for describing the movement behavior of tunas in FAD arrays.
386 The model is built upon four main behavioral components, based on the state-of-the-art knowledge
387 of the associative dynamics of tunas at FADs: random walk dynamics, orientation capabilities, diel
388 behavior and a lack in correlation between the duration of consecutive CRTs and CATs. A relatively
389 small number of parameters drive the model's properties: swimming speed, path sinuosity, orientation
390 radius and mortality rate. Despite the model's structural simplicity and the reduced number of
391 parameters, it was able to reproduce both of the investigated movement metrics (time between two
392 FAD associations and total time spent in the array) in two different FAD arrays.
393 The four parameters tested can be related to the physiological capabilities and condition of tuna, as
394 well as their environment (including the FADs, other tuna and non-tuna species present in the array).
395 The two swimming speeds tested (corresponding to the 0.7 and 1.4 m/s) stem from previous studies
396 showing that swimming speed typically range between 1 and 2 body lengths per second (Girard et
397 al., 2004; Dagorn et al. 2013b). In contrast, despite previous evidences of a random walk behavior in
398 tuna movements between FADs (Girard et al. 2004; Pérez et al. 2020), no empirical studies have
399 estimated the sinuosity of a tuna path in a FAD array. As a consequence, large ranges of sinuosity
400 were considered. The results show that, while both speed values could be retained by the simulations,
401 only a limited subset of sinuosity coefficients emerged. The majority of sinuosity coefficients that
402 were retained indicated a rather skewed distribution of turning angles (Fig. 3, Table 3). Lower
403 sinuosity coefficients were mostly found for the highest swimming speed (Table 3). This is to be
404 expected considering that for a given average distance traveled during a correlated random walk,
405 higher speeds imply lower sinuosity coefficients and vice-versa (Hall 1977; Kareiva & Shigesada
406 1983; Marsh & Jones 1988). Hence, the values of the sinuosity coefficient (c) retained are valid
407 considering the chosen time step (Δt=100 s). It is likely that the tuna movement characteristics (speed
408 and sinuosity) also depend on the fine-scale environmental characteristics within the FAD array, such
409 as the type and distribution of prey, or the physiological conditions of the tuna itself. In future, the
410 consideration of a range of swimming speeds and path sinuosity, as opposed to single values, could
411 provide a more realistic picture of tuna movements. However, the range of values used in this study
412 provides an initial set of movement characteristics that are compatible with field observations, thus
413 contributing to the poorly understood dynamics of tuna in a FAD array.
414 The mortality rate (which accounts for both natural and fishing mortality) is primarily influenced by
415 risks associated with fishing activity, natural predation and disease. A previous study using
416 conventional tags from the Hawaii Tuna Tagging Project (HTTP) showed a natural mortality rate of
417 0.36% per day and a fishing mortality of 0.67 % per day for yellowfin tuna larger than 56 cm (Adam
418 et al. 2003). As such, the global mortality rates estimated through our simulations appear to be higher

than previous findings. This difference could be due to a specific mortality in each study site and period considered. Indeed, even if in both cases the Hawaiian archipelago was considered, these studies concern different islands and study periods, for which the fishing pressure might differ as well as the natural mortality.

Acoustic telemetry data do not allow for the direct estimation of mortality rate, but do provide information on the time at which an individual is no longer detected by receivers deployed on FADs. Generally, a lack of acoustic detections indicates that tuna have either left the FAD array or died. Movement dynamics of tuna can explain the first potential causes for a lack of detection. Within the model, the propensity of an individual to depart from the array is directly linked to the sinuosity of its path, its swimming speed and its orientation radius. For instance, large path sinuosity (resulting from small values of the sinuosity coefficient c) primarily leads to movements close to the FAD of departure and little or no detections at the other FADs. Conversely, small path sinuosity (form high values of the coefficient of sinuosity c) generally results in individuals rapidly leaving the array (Fig. 3 and Supplementary Information 1). In this way, the model provides direct information on the rate at which tuna are lost from FAD arrays. Fitting the model to the field data allows for differentiation between loss through randomness of movement and loss due to mortality (Table 2 and Supplementary Information 3). As such this field-based movement model could provide a new and alternative methodology for estimating the mortality rates of tuna in a FAD array.

In the model, the orientation radius represents the distance from which tunas are able to orient themselves towards FADs them, while on the field tuna could be able to perceive FADs before orienting themselves toward them. No data is available on the distance at which tunas perceive FADs, but tuna movements provide input on the distance at which tunas start to orient themselves toward FADs. Therefore, the FAD perception radius was not considered in this study. This distance naturally depends on the tuna's ability to perceive its surrounding environment, as well as on the physical characteristics of the area. Given the large distances from which tuna can orient themselves towards FADs, highlighted in previous studies (Girard et al. 2004), as well as those found in this study, the use of visual cues as explanatory factors can be discarded. As sound can travel great distances underwater, the perception of acoustic stimuli could be a valid hypothesis for explaining the ability of tunas to orient towards FADs from such large distances. Environmental characteristics may impact the propagation of sounds between FADs and tunas and influence how strong these sound stimuli are. The physical characteristics of the water mass are known to affect the propagation of sound waves (Lee et al. 2017; Siddiqui & Dong 2019). Furthermore, the topology of the FAD array and its location relative to the coastline could also affect underwater sound propagation. As sounds may be produced by the FAD structures themselves, they can vary depending on the materials used and the design of each structure, which often differ among FAD arrays. Although FAD design has not been identified

as influencing the attractiveness of FADs (Fréon & Dagorn 2000), it may impact their detectability. Tunas may also perceive the presence of a FAD through the emission of noise generated by the fish aggregation itself. In such a situation the intensity of the noise could be dependent on the quantity of fish present, but also on the types of species and their activities. Considering these multiple potential sources of environmental variability, the distance at which tuna are able to perceive FADs (orientation radius) is likely to vary both within and between FAD arrays. No single value of the orientation radius can exist, but rather a distribution of these distances with a subset of values for which the probability of being located in the environment is greatest. A general model that describes the movements of tuna in different FAD arrays with the same parameters, such as the one developed in this study, provides a subset of the most probable orientation distances. However, it is likely that a distribution of orientation distances could be more realistic and for a particular FAD, the orientation radius could have its own dynamics according to local environmental conditions.

A previous study by Girard et al. (2004) determined orientation radii between 4 and 17 km, with a mode around 10 km. This study was based on 14 yellowfin tuna (YFT) from 47 cm to 167 cm FL, that were acoustically tracked in different FAD arrays (Holland et al., 1990; Marsac & Cayré, 1998; Brill et al. 1999; Dagorn et al. 2000) and included the specie-size category considered in our simulations (YFT of ~70 cm). These 14 individuals were actively tracked over short durations, between 12 and 86 hours (due to the constraints of active tracking) rather than passively monitored as in our study. The radii found in our 7 sets of parameters (5 km and 2 km in one set) are similar to the lower range of the orientation distances (4-17 km) found by Girard et al. (2004). The longer orientation distances identified in that study could be attributed to the inclusion of only long paths (more than 7 km away from the FADs) in their analysis. Furthermore, the authors considered that the longest orientation distances (e.g. > 15 km) could be the result of tuna patrolling along the coast, thus using some bathymetric information rather than signals from FADs. As such, the distances found by Girard et al. (2004) may represent maximum orientation distances, while the average could be shorter, and more similar to the values we found (2-5 km).

Finally, it is important to note that the two studies considered different datasets collected in different regions, and possible inter-FAD array variability in the orientation radius cannot be excluded. It is important to stress that the retention of the model parameters was very conservative: only those valid for both metrics (TRT and CATdiff) and FAD arrays were kept. In doing so, possible local variability in tuna behavior (for example, a different orientation radius depending on the study site) were excluded. This choice was made to obtaining the minimal, and most general model, that could reproduce the observations. Considering a threshold of 85% for the percentage of retained bootstraps provides 7 sets of parameter values over the 648 tested. These values (radius of orientation ranging between 2-5 km, coefficient of sinuosity between 0.9 and 0.995, mortality rates between 2 and 3%)

provide the main characteristics of tuna movements in FAD arrays. To avoid any scaling issue, the same data treatment was applied to both field and simulated data sets. Therefore, the model can be considered to correctly reproduce the tuna movements between FADs at the dayscale, i.e., the scale related to a maximum blanking period of 24h (Capello et al. 2015), which was used to process the acoustic data. Further studies, across a greater number of study sites, could provide insight into how these model parameters could vary between FAD arrays. Similarly, it would be of interest to consider how this model, fitted for YFT-70, is able to describe the behavior of other tuna species and sizes. This model could also be used for other non-tuna species that associate with FADs and in particular vulnerable species such as the silky sharks (*Carcharhinus falciformis*).

As this model aimed to simulate tuna movements in FAD arrays, the time tuna spent associated with FADs (CRT) was not simulated and the experimental CRT distribution was used as an input of the model. Further model developments, which consider social interactions at FADs (Robert et al. 2014; Pérez et al. 2020), may allow the CRT durations within different FAD arrays to also be integrated into the model. This integration of CRTs into the model would involve adding social interactions between individuals and behavioral rules of social retention at the FAD that follow the meeting point hypothesis (Dagorn & Fréon 1999, Fréon & Dagorn, 2000, Robert el al. 2014).

5. Conclusion

Building on current knowledge of the associative behavior tuna at FADs from acoustic telemetry data, our model is the first to reproduce the movement behavior of tunas in a FAD array. A total of 7 sets of parameters (Table 3) were able to reproduce, with a high confidence, the movements of yellowfin tuna (fork length 70 cm) in two different FAD arrays, suggesting the model is robust. Future model improvements could consider distributions of speeds, sinuosity, detection radii and mortality rates (rather than fixed values) which may provide a better reflection of the variability induced by the local environment and the physiological conditions of the tuna themselves.

This model can be used on all species that display associative behavior with floating object. This includes species such as dolphinfish (*Coryphaena hippurus*) or the vulnerable silky shark (*Carcharhinus falciformis*). When combined with acoustic telemetry data, the model can provide an alternative method for determining the mortality rate of tuna and other associated species in a FAD array. Given the difficulty in assessing natural and fishing mortality for wild marine species, this novel approach could be of interest for the stock assessment community. Moreover, the model could be used to predict how increasing numbers of FADs affect the ecology of tunas ecology, both in terms of the time spent away from FADs and the total time spent in a FAD array. This study offers a new tool to provide science-based advice for the management of FAD fisheries, since the more time fish

spend associated, the more vulnerable these individuals are to the fishery. Scenarios could be extended to drifting FADs in open ocean areas, as both anchored and drifting FADs alter the environment in a similar way (Dagorn et al. 2010). While acoustic telemetry experiments have successfully characterized residence times at drifting FADs (Govinden et al. 2010; Forget et al. 2015), measuring in situ absence times of tunas within drifting FAD arrays is a major research challenge and these parameters are key for the development of robust FAD management plans by Tuna Regional Fisheries Management Organisations (RFMOs). Our model provides a method for estimate these parameters in the absence of data from acoustically tagged tuna in drifting FAD arrays.

Finally, the same approach can be used to study the movement behavior of other marine and terrestrial species that manifest an associative behavior with aggregating sites, and for which presence/absence data are recorded at these sites. For instance, our model could be used to study the movements of terrestrial animals who show associative behaviors with waterholes (Zvidzai et al. 2013; O'Farrill et al. 2014) detected through camera traps (Swann & Perkins, 2014; Hughey et al. 2018.). More generally, this method could be used even without any associative behavior at specific sites, as long as the study site is equipped with regularly spaced and sufficiently numerous receivers where individuals can be identified.

Data Availibity Statement

Simulations were performed with the model FAT albaCoRaW v1.3. All scripts and data used in this study are available on GitHub (https://github.com/adupaix/FAT_albaCoRaW, doi: 10.5281/zenodo.5834056.).

Acknowledgements

The authors would like to acknowledge the two anonymous reviewers for their extensive and constructive feedback.

Funding

This project was co-funded by the ANR project BLUEMED (ANR-14-ACHN-0002), "Observatoire des Ecosystèmes Pélagiques Tropicaux exploités" (Ob7) from IRD/MARBEC and by the International Pole-and-line Foundation (IPNLF).

Authors' contributions

SB, KH and LD collected the raw data in the field. GP developed the model, with major contribution of AD and MC. GP analysed the data and wrote the paper with major contribution of MC, LD, JLD and AD. All authors read and approved the final manuscript.

Bibliography

Adam, M. S., Sibert, J., Itano, D., & Holland, K. (2003). Dynamics of bigeye (Thunnus obesus) and yellowfin (T. albacares) tuna in Hawaii's pelagic fisheries: Analysis of tagging data with a bulk transfer model incorporating size-specific attrition. *Fishery Bulletin*, *101*(2), 215–228.

Ahearn, S. C., Dodge, S., Simcharoen, A., Xavier, G., & Smith, J. L. D. (2017). A context-sensitive correlated random walk: a new simulation model for movement. *International Journal of Geographical Information Science*, *31*(5), 867–883. https://doi.org/10.1080/13658816.2016.1224887

Benhamou, S. (2004). How to reliably estimate the tortuosity of an animal's path: Straightness, sinuosity, or fractal dimension? *Journal of Theoretical Biology*, *229*(2), 209–220. https://doi.org/10.1016/j.jtbi.2004.03.016

Bovet, P., & Benhamou, S. (1988). Spatial analysis of animals' movements using a correlated random walk model. *Journal of Theoretical Biology*, *131*(4), 419–433. https://doi.org/10.1016/S0022-5193(88)80038-9

Brill, R. W., Block, B. A., Boggs, C. H., Bigelow, K. A., Freund, E. V, & Marcinek, D. J. (1999). Horizontal movments and depth distribution of large adult yellowfin tuna (Thunnus albacares) near the Hawaiian Islands, recorded using ultrasonic telemetry: implications for hte physiological ecology of pelagic fishes. *Marine Biology*, *133*, 395–408. https://doi.org/10.1007/s002270050478

Byers, J. A. (2001). Correlated random walk equations of animal dispersal resolved by simulation. *Ecology*, *82*(6), 1680–1690. https://doi.org/10.1890/0012-9658(2001)082[1680:CRWEOA]2.0.CO;2

Capello, M., Robert, M., Soria, M., Potin, G., Itano, D., Holland, K., … Dagorn, L. (2015). A methodological framework to estimate the site fidelity of tagged animals using passive acoustic telemetry. *PLoS ONE*, *10*(8), 1–19. https://doi.org/10.1371/journal.pone.0134002

Carita M., B., James A., S., & S.N., L. (2000). Caribou movement as a correlated random walk. *Oecologia*, *123*, 364–374.

Castro, J., Santiago, J., & Santana-Ortega, T. (2002). A general theory on fish aggregation to floating objects: An alternative to the meeting point hypothesis. *Reviews in Fish Biology and Fisheries*, *11*, 255–277. https://doi.org/10.1023/A:1020302414472

Codling, E. A., Plank, M. J., & Benhamou, S. (2008). Random walk models in biology. *Journal of the Royal Society Interface*, *5*(25), 813–834. https://doi.org/10.1098/rsif.2008.0014

Cramer, A., Katz, S., Kogan, C., & Lindholm, J. (2021). Distinguishing residency behavior from random movements using passive acoustic telemetry. *Marine Ecology Progress Series*, *672*, 73–87. https://doi.org/10.3354/meps13760

Dagorn, L., & Fréon, P. (1999). Tropical tuna associated with floating objects: a simulation study of the meeting point hypothesis. *Canadian Journal of Fisheries and Aquatic Sciences*, *56*(6), 984–993. https://doi.org/10.1139/cjfas-56-6-984

598 Dagorn, L., Holland, K. N., Restrepo, V., & Moreno, G. (2013a). Is it good or bad to fish with
599 FADs? What are the real impacts of the use of drifting FADs on pelagic marine ecosystems?
600 Fish and Fisheries, 14(3), 391–415. https://doi.org/10.1111/j.1467-2979.2012.00478.x

601 Dagorn, L., Bez, N., Fauvel, T., & Walker, E. (2013b). How much do fish aggregating devices
602 (FADs) modify the floating object environment in the ocean? *Fisheries Oceanography*, *22*(3),
603 147–153. https://doi.org/10.1111/fog.12014

604 Dagorn, L., Holland, K. N., & Filmalter, J. D. (2010). Are drifting FADs essential for testing the
605 ecological trap hypothesis? *Fisheries Research*, *106*(1), 60–63.
606 https://doi.org/10.1016/j.fishres.2010.07.002

607 Dagorn, L., Holland, K. N., & Itano, D. (2007). Behavior of yellowfin (Thunnus albacares) and
608 bigeye (T. obesus) tuna in a network of fish aggregating devices (FADs). *Marine Biology*,
609 *151*(2), 595–606. https://doi.org/10.1007/s00227-006-0511-1

610 Dagorn, L., Holland, K. N., Restrepo, V., & Moreno, G. (2013). Is it good or bad to fish with FADs?
611 What are the real impacts of the use of drifting FADs on pelagic marine ecosystems? *Fish and*
612 *Fisheries*, *14*(3), 391–415. https://doi.org/10.1111/j.1467-2979.2012.00478.x

613 Dagorn, L., Josse, E., Bach, P., & Bertrand, A. (2000). Modeling tuna behaviour near floating
614 objects: From individuals to aggregations. *Aquatic Living Resources*, *13*(4), 203–211.
615 https://doi.org/10.1016/S0990-7440(00)01065-2

616 Dempster, T., & Taquet, M. (2004). Fish aggregation device (FAD) research: Gaps in current
617 knowledge and future directions for ecological studies. *Reviews in Fish Biology and Fisheries*,
618 *14*(1), 21–42. https://doi.org/10.1007/s11160-004-3151-x

619 Elzhov T.V., Mullen K. M., Spiess, A-N., & Bolker, B. (2016). minpack.lm: R Interface to the
620 Levenberg-Marquardt Nonlinear Least-Squares Algorithm Found in MINPACK, Plus
621 Support for Bounds. R package version 1.2-1. https://CRAN.R-
622 project.org/package=minpack.lm

623 Forget, F., Capello, M., Filmalter, J. D., Govinden, R., Soria, M., Cowley, P. D., & Dagorn, L.
624 (2015). Behaviour and vulnerability of target and non-target species at drifting fish aggregating
625 devices (FADs) in the tropical tuna purse seine fishery determined by acoustic telemetry.
626 *Canadian Journal of Fisheries and Aquatic Sciences*, *72*(9), 1398–1405.
627 https://doi.org/10.1139/cjfas-2014-0458

628 Fréon, P., & Dagorn, L. (2000). Review of fish associative behaviour: Toward a generalisation of
629 the meeting point hypothesis. *Reviews in Fish Biology and Fisheries*, *10*(2), 183–207.
630 https://doi.org/10.1023/A:1016666108540

631 Girard, C., Benhamou, S., & Dagorn, L. (2004). FAD: Fish Aggregating Device or Fish Attracting
632 Device? A new analysis of yellowfin tuna movements around floating objects. *Animal*
633 *Behaviour*, *67*(2), 319–326. https://doi.org/10.1016/j.anbehav.2003.07.007

634 Girard, C., Dagorn, L., Taquet, M., Aumeeruddy, R., Peignon, C., & Benhamou, S. (2007). Homing
635 abilities of dolphinfish (Coryphaena hippurus) displaced from fish aggregating devices (FADs)
636 determined using ultrasonic telemetry . Aquatic Living Resources, 321(2007), 313–321.
637 https://doi.org/10.1051/alr:2008005

Govinden, R., Capello, M., Forget, F., Filmalter, J. D., & Dagorn, L. (2021). Behavior of skipjack (*Katsuwonus pelamis*), yellowfin (*Thunnus albacares*), and bigeye (*T. obsesus*) tunas associated with drifting fish aggregating devices (dFADs) in the Indian Ocean, assessed through acoustic telemetry. *Fisheries Oceanography*. https://doi.org/10.1111/fog.12536

Govinden, R., Dagorn, L., Soria, M., & Filmalter, J. (2010). Behaviour of Tuna associated with Drifting Fish Aggregating Devices (FADs) in the Mozambique Channel, 1–22.

Govinden, R., Jauhary, R., Filmalter, J. D., Forget, F., Soria, M., Adam, M. S., & Dagorn, L. (2013). Movement behaviour of skipjack (Katsuwonus pelamis) and yellowfin (Thunnus albacares) tuna at anchored fish aggregating devices (FADs) in the Maldives, investigated by acoustic telemetry. *Aquatic Living Resources*, *26*(1), 69–77. https://doi.org/10.1051/alr/2012022

Hall, R. L. (1977). Amoeboid Movement as a Correlated Walk. *Journal of Mathematical Biology*, *4*, 327–335. https://doi.org/10.1177/1077546311406307

Hall, M. A. (1992). The association of tunas with floating objects and dolphins in the Eastern Pacific ocean: VII. Some hypotheses on the mechanisms governing the association of tunas with floating objects and dolphins. *Backgound Document for the International Workshop on the Ecology and Fisheries for Tunas Associated with Floating Objects, February 11-13 1992, La Jolla, CA*, *January*, 6.

Holland, K. N., Brill, R. W., & Chang, R. K. C. (1990). Horizontal and vertical movements of yellowfin and bigeye tuna associated with fish aggregating devices. *Fishery Bulletin*, *88*(3), 493–507.

Hughey, L. F., Hein, A. M., Strandburg-Peshkin, A., & Jensen, F. H. (2018). Challenges and solutions for studying collective animal behaviour in the wild. *Philosophical Transactions of the Royal Society B: Biological Sciences*, *373*(1746), 1–13. https://doi.org/10.1098/rstb.2017.0005

Josse, E., Dagorn, L., & Bertrand, A. (2000). Typology and behaviour of tuna aggregations around fish aggregating devices from acoustic surveys in French Polynesia. *Aquatic Living Resources*, *13*(4), 183–192. https://doi.org/10.1016/S0990-7440(00)00051-6

Kareiva, P. M., & Shigesada, N. (1983). Analyzing Insect Movement as a Correlated Random Walk. *Oecologia*, *56*(2), 234–238.

Lee, K. M., Ballard, M. S., McNeese, A. R., & Wilson, P. S. (2017). Sound speed and attenuation measurements within a seagrass meadow from the water column into the seabed. *The Journal of the Acoustical Society of America*, *141*(4), 402–406. https://doi.org/10.1121/1.4979302

Marsac, F., & Cayré, P. (1998). Telemetry 'applied to behaviour analysis of yellowfin tuna (Thunnus albacares, Bonnaterre, 1788) movements in a network of fish aggregating devices. *Hydrobiologia*, (May 1998), 155–171. https://doi.org/10.1023/A

Marsac, F., Fonteneau, A., & Ménard, F. (2000). Drifting FADs used in tuna fisheries: an ecological trap? *Biologie and Behaviour of Pelagic Fish Aggreagtions*, 537–552.

Marsh, L. M., & Jones, R. E. (1988). The form and consequences of random walk movement models. *Journal of Theoretical Biology*, *133*(1), 113–131. https://doi.org/10.1016/S0022-5193(88)80028-6

McClintock, B. T., King, R., Thomas, L., Matthiopoulos, J., McConnell, B. J., & Morales, J. M. (2012). A general discrete-time modeling framework for animal movement using multistate random walks. *Ecological Monographs*, *82*(3), 335–349. https://doi.org/10.1890/11-0326.1

Moreno, G., Dagorn, L., Sancho, G., & Itano, D. (2007). Fish behaviour from fishers' knowledge: the case study of tropical tuna around drifting fish aggregating devices (DFADs). *Canadian Journal of Fisheries and Aquatic Sciences*, *64*(11), 1517–1528. https://doi.org/10.1139/f07-113

Murua, H., Dagorn, L., Justel-Rubio, A., Moreno, G. and Restrepo, V. (2021). Questions and Answers about FADs and Bycatch (Version 3). ISSF Technical Report 2021-11. International Seafood Sustainability Foundation, Washington, D.C., USA

O'Farrill G, Schampaert KG, Rayfield B, Bodin Ö, Calmé S, Sengupta R,Gonzalez A. The potential connectivity of waterhole networks and theeffectiveness of a protected area under various drought scenarios. PLoSOne. 2014;9(5).https://doi.org/10.1371/journal.pone.0095049

Ohta, I., & Kakuma, S. (2005). Periodic behavior and residence time of yellowfin and bigeye tuna associated with fish aggregating devices around Okinawa Islands, as identified with automated listening stations. *Marine Biology*, *146*(3), 581–594. https://doi.org/10.1007/s00227-004-1456-x

Palencia, P., Rowcliffe, J. M., Vicente, J., & Acevedo, P. (2021). Assessing the camera trap methodologies used to estimate density of unmarked populations. *Journal of Applied Ecology*, *58*(8), 1583–1592. https://doi.org/10.1111/1365-2664.13913

Papastamatiou, Y. P., Meyer, C. G., Carvalho, F., Dale, J. J., Hutchinson, M. R., & Holland, K. N. (2013). Telemetry and random-walk models reveal complex patterns of partial migration in a large marine predator. In *Ecology* (Vol. 94, Issue 11).

Patterson, T. A., Basson, M., Bravington, M. V., & Gunn, J. S. (2009). Classifying movement behaviour in relation to environmental conditions using hidden Markov models. *Journal of Animal Ecology*, *78*(6), 1113–1123. https://doi.org/10.1111/j.1365-2656.2009.01583.x

Pedro G. Lino, LLuıs Bentes, David Abecasis, Miguel Neves dos Santos, & Karim Erzini. (2009). *Tagging and Tracking of Marine Animals with Electronic Devices* (J. L. Nielsen, H. Arrizabalaga, N. Fragoso, A. Hobday, M. Lutcavage, & J. Sibert, Eds.; Vol. 9). Springer Netherlands. https://doi.org/10.1007/978-1-4020-9640-2

Pérez, G., Dagorn, L., Deneubourg, J., Forget, F., Filmalter, J. D., Holland, K., … Capello, M. (2020). Effects of habitat modifications on the movement behavior of animals : the case study of Fish Aggregating Devices (FADs) and tropical tunas. *Movement Ecology*, *8*(47), 1–10.

Robert, M., Dagorn, L., & Deneubourg, J. L. (2014). The aggregation of tuna around floating objects: What could be the underlying social mechanisms? *Journal of Theoretical Biology*, *359*(October), 161–170. https://doi.org/10.1016/j.jtbi.2014.06.010

Robert, M., Dagorn, L., Filmalter, J. D., Deneubourg, J. L., Itano, D., & Holland, K. (2013). Intra-individual behavioral variability displayed by tuna at fish aggregating devices (FADs). *Marine Ecology Progress Series*, *484*, 239–247. https://doi.org/10.3354/meps10303

Rodriguez-Tress, P., Capello, M., Forget, F., Soria, M., Beeharry, S. P., Dussooa, N., & Dagorn, L. (2017). Associative behavior of yellowfin Thunnus albacares, skipjack Katsuwonus pelamis,

and bigeye tuna T. obesus at anchored fish aggregating devices (FADs) off the coast of Mauritius. *Marine Ecology Progress Series*, *570*, 213–222. https://doi.org/10.3354/meps12101

Romanov, E. V. (2002). By catch in the tuna purse-seine fisheries of the western Indian Ocean. Fishery Bulletin, 100(1), 90–105.

Scott, G. P., & Lopez, J. (2014). The use of FADs in tuna fisheries.

Siddiqui, S. I., & Dong, H. (2019). Effects of Water Column Variations on Sound Propagation and Underwater Acoustic Communications. *Sensors (Basel, Switzerland)*, *19*(9). https://doi.org/10.3390/s19092105

South, A. (2011). rworldmap: A New R package for Mapping Global Data. *The R Journal*, *3*(1), 35–43.

Swann, D. E., & Perkins, N. (2014). Camera trapping for animal monitoring and management: a review of applications. In *Camera Trapping* (pp. 3–11).

Taquet, M., Sancho, G., Dagorn, L., Gaertner, J.-C., Itano, D., Aumeeruddy, R., Wendling, B., & Peignon, C. (2007). Characterizing fish communities associated with drifting fish aggregating devices (FADs) in the Western Indian Ocean using underwater visual surveys. Aquatic Living Resources, 21(4), 331–341. https://doi.org/Doi 10.1051/Alr:2008007

Therneau, T. M., & Grambsch, P. M. (2000). Modeling Survival Data: Extending the Cox Model. *Springer*.

Tolotti, M. T., Forget, F., Capello, M., Filmalter, J. D., Hutchinson, M., Itano, D., … Dagorn, L. (2020). Association dynamics of tuna and purse seine bycatch species with drifting fish aggregating devices (FADs) in the tropical eastern Atlantic Ocean. *Fisheries Research*, *226*(June 2019), 105521. https://doi.org/10.1016/j.fishres.2020.105521

Zvidzai M, Murwira A, Caron A, de Garine-Wichatitksy M. Waterhole usepatterns at the wildlife/livestock interface in a semi-arid savanna ofsouthern Africa. Int J Dev Sustain. 2013;2(2):455–71